RSC Advances

PAPER

View Article Online
View Journal | View Issue

Cite this: *RSC Adv.*, 2026, **16**, 26222

Comparative evaluation of donepezil-loaded polymeric and liposomal nanoparticles for Alzheimer's disease: biocompatibility, drug release kinetics, and cellular uptake study

Toros Torossian, †[a] Kawthar K. Abla, †[b] Jana Dakour, [ce] Sara Assi, [c] Mia Karam [cd] and Rami Mhanna *[c]

Alzheimer's disease (AD) is a neurodegenerative condition that accounts for approximately 65% of all dementia cases worldwide. Donepezil (DNP) is an acetylcholinesterase inhibitor that is widely prescribed for AD patients. However, extensive first-pass metabolism and the presence of the blood–brain barrier (BBB) significantly restrict its therapeutic efficacy. To address these challenges, two nanocarrier systems were developed: biodegradable polycaprolactone (PCL) and polyvinyl alcohol (PVA)-based polymeric nanoparticles, and dipalmitoylphosphatidylcholine (DPPC)-based liposomes. DNP-loaded PCL/PVA double emulsion nanoparticles and DPPC liposomes were prepared and characterized based on their particle sizes, uniformity, zeta potential, entrapment efficiency, Fourier transform infrared spectroscopy (FTIR), and *in vitro* drug release kinetics. Their safety profiles and cellular uptake potential were evaluated using the trypan blue exclusion assay and qualitative and quantitative cellular uptake assays with the human endothelial-like ECV-304 and neuronal PC-12 cell lines. The mean particle sizes of polymeric nanoparticles and liposomes were 175.97 ± 11.72 nm and 115.18 ± 4.63 nm, respectively, with low polydispersity indices (<0.3) and negative zeta potentials. FTIR analysis confirmed the absence of chemical interactions between DNP and formulation components. In addition, both nanocarrier systems demonstrated favorable biocompatibility, with cell viability exceeding 80%. Liposomes exhibited a more controlled drug release profile over 48 hours compared to polymeric nanoparticles. In contrast, both formulations exhibited significantly higher cellular uptake compared to their respective controls, with polymeric nanoparticles showing significantly higher cellular uptake than liposomes in ECV-304 cells (27.41 ± 2.38%, $p < 0.05$), demonstrating that carrier composition is a key determinant of nanoparticle–cell interactions independent of targeting ligands or surface modifications. This suggests that polymeric nanoparticles enhance *in vitro* cellular uptake in endothelial-like cells, warranting further *in vivo* investigation for their brain delivery potential.

Received 3rd February 2026
Accepted 10th May 2026

DOI: 10.1039/d6ra00929h

rsc.li/rsc-advances

1. Introduction

Alzheimer's disease (AD) is a neurodegenerative disorder that affects millions of people worldwide.[1] AD is the most common cause of dementia, affecting around 7.2 million of the older population in the United States, and this number is projected to increase to 13.8 million by 2060 without significant medical breakthroughs in the prevention or treatment of the disease.[2] Although the exact cause of AD remains unclear, oxidative stress, dysregulated metal homeostasis, and neuroinflammation have all been implicated in its etiology. Donepezil hydrochloride (DNP; (±)-2-[(1-benzylpiperidin-4-yl)methyl]-5,6-dimethoxyindan-1-one monohydrochloride) is a reversible cholinesterase inhibitor with high specificity for active acetylcholinesterase in the central nervous system (CNS). DNP is commonly prescribed to improve memory performance and cognitive function in patients with dementia. It acts by inhibiting acetylcholinesterase activity, thereby increasing acetylcholine levels in the remaining brain neurons, which in turn improves cholinergic neurotransmission and cognitive

[a]*Biomedical Engineering Program, Maroun Semaan Faculty of Engineering and Architecture, American University of Beirut, Beirut, 1107 2020, Lebanon*

[b]*Pharmaceutical Nanotechnology Research Lab, Faculty of Pharmacy, Beirut Arab University, Beirut, Lebanon*

[c]*Biomedical Engineering Program, Maroun Semaan Faculty of Engineering and Architecture, American University of Beirut, Beirut, 1107 2020, Lebanon. E-mail: rm136@aub.edu.lb; Tel: +9613/080865*

[d]*Department of Biochemistry and Molecular Genetics, Faculty of Medicine, American University of Beirut, Beirut, Lebanon*

[e]*Department of Immunology, The University of Texas Southwestern Medical Center, Dallas, TX 75390, USA*

† These authors contributed equally to the work.

performance.[3] Until recently, DNP was only commercially available as orally administered tablets approved by the U.S. Food and Drug Administration (FDA). Nevertheless, the high first-pass metabolism of DNP, combined with the presence of the blood–brain barrier (BBB), significantly reduces the amount of drug reaching the site of action. This necessitates the use of higher doses of DNP to achieve and maintain a therapeutic effect in the brain. As a result, patients experience more peripheral adverse events that are mainly associated with cholinergic functions (nausea, diarrhea, dizziness, and insomnia), causing low compliance with treatment.[4] Consequently, developing an effective, safe, and affordable drug delivery system is crucial to enhancing the therapeutic efficacy of DNP in AD.[5]

Nanocarrier drug delivery systems have emerged as a promising approach to overcoming biological barriers and addressing the limitations of conventional drug formulations.[6,7] Nanoparticles (NPs), typically less than 1000 nm in size, augment pharmacokinetic properties and exhibit high stability in biological environments due to their small size. These features enhance cellular uptake and drug delivery to the brain, allowing them to more readily penetrate the BBB and reach the desired brain regions.[8,9] Furthermore, systemic toxicity is a major concern that must be considered when traditional drug administration methods are employed to deliver therapeutics to the brain. This limitation can be significantly overcome using NPs for a more controlled and sustained release of therapeutic compounds, thereby limiting their potential toxic adverse effects. Several studies have focused on the intranasal administration of DNP-loaded NPs through the nasal cavity, which bypasses the BBB; however, the low permeability of the nasal mucosa, along with excessive mucociliary clearance, necessitates frequent administration, which irritates the nasal cavity in the long term.[10] In contrast, oral administration of nanoparticle formulations protects the encapsulated drug from gastrointestinal degradation and enhances the absorption and transport of the NPs through the gastrointestinal tract, ultimately improving oral bioavailability and making oral administration a more viable route for sustained delivery of DNP.[11]

There are different types of nanocarriers. Inorganic nanocarriers, exemplified by quantum dots and metal-based NPs, can be modified to achieve desirable physicochemical properties; thus, several studies have reported their successful use in drug delivery across the BBB.[12] Nevertheless, concerns about their adverse effects, such as *in vivo* retention and biotoxicity, remain unresolved. Therefore, their use in clinical applications has remained limited. On the other hand, organic materials, such as lipid- and biodegradable polymer-based NPs, have demonstrated relatively better biocompatibility and are being extensively investigated worldwide.[13] These NPs offer several advantages, including surface modifications for targeted delivery, encapsulation of both hydrophilic and hydrophobic drugs, prolonging drug release, and protection of encapsulated cargoes against harsh biological environments.[14] Furthermore, the small size of these NPs has been shown to facilitate their transport across the BBB through endocytosis, lipid exchange, or fusion.[9]

Nanocarrier-based formulations of DNP, including polymeric NPs and liposomal systems, have been developed and individually optimized in previous studies for improved drug delivery and therapeutic performance. For instance, DNP-loaded PLGA nanoparticles and ApoE3-conjugated mPEG-PCL polymeric nanoparticles have demonstrated brain-targeting potential.[15,16] Similarly, DNP-loaded and chitosan-coated phosphatidylcholine liposomes have shown enhanced BBB penetration *in vivo*.[17] However, these systems have been evaluated separately under different experimental conditions, including distinct polymer compositions, routes of administration, and cell lines. Consequently, direct comparative studies under standardized conditions have not been conducted, and whether carrier composition influences cellular uptake and release kinetics independently of other variables remains to be determined.

Given this, the current work aims to determine whether carrier material composition affects endothelial and neuronal uptake. For this purpose, DNP-loaded polymeric NPs composed of biodegradable polycaprolactone (PCL) and polyvinyl alcohol (PVA) were prepared through double emulsion, and a 1,2-dipalmitoyl-*sn*-glycero-3-phosphocholine (DPPC)-based liposomal system was also prepared for side-by-side comparison under identical experimental conditions. The two delivery systems were characterized in terms of particle size, polydispersity index (PDI), zeta potential, entrapment efficiency, *in vitro* drug-release kinetics, and morphological properties. In addition, biocompatibility was assessed using the trypan blue exclusion assay. Finally, cellular uptake of the two systems was evaluated both qualitatively and quantitatively in endothelial and neuronal cell models.

2. Materials and methods

2.1. Materials

Polycaprolactone (average M_W 80 000 Da), poly(vinyl alcohol) (M_W 13 000–23 000 Da, 87–89% hydrolyzed), dichloromethane (DCM), cholesterol, Roswell Park Memorial Institute (RPMI-1640) and Dulbecco's Modified Eagle Medium/Nutrient Mixture F-12 (DMEM/F-12, Ham) cell culture medium, fetal bovine serum (FBS), trypsin enzyme, 0.4% trypan blue solution, and sterile phosphate-buffered saline (PBS) were purchased from Sigma-Aldrich (St. Louis, MO, USA). 1,2-Dipalmitoyl-*sn*-glycero-3-phosphocholine (DPPC), 18 : 1 Liss Rhod PE (1,2-dioleoyl-*sn*-glycero-3-phosphoethanolamine-*N*-(lissamine rhodamine B sulfonyl) ammonium salt), and 10 mm filter supports were obtained from Avanti Polar Lipids. Whatman Nuclepore polycarbonate membrane filters (pore size: 0.1 μm) were purchased from Cytiva (Marlborough, MA, USA). Paraformaldehyde (90%, pure) and FITC-Avidin (0.1% sodium azide) were purchased from Acros Organics (Thermo Fisher Scientific Inc., USA). Penicillin–streptomycin was obtained from Biowest (Nuaille, France), and Triton X-100 was acquired from Genesee Scientific (USA). Donepezil hydrochloride was kindly donated by Benta Pharma Industries (Lebanon). All other chemicals and solvents used were of analytical grade.

The human endothelial-like cell line ECV-304 and the immortalized rat-derived neuronal-like cell line PC-12 were purchased from ATCC.

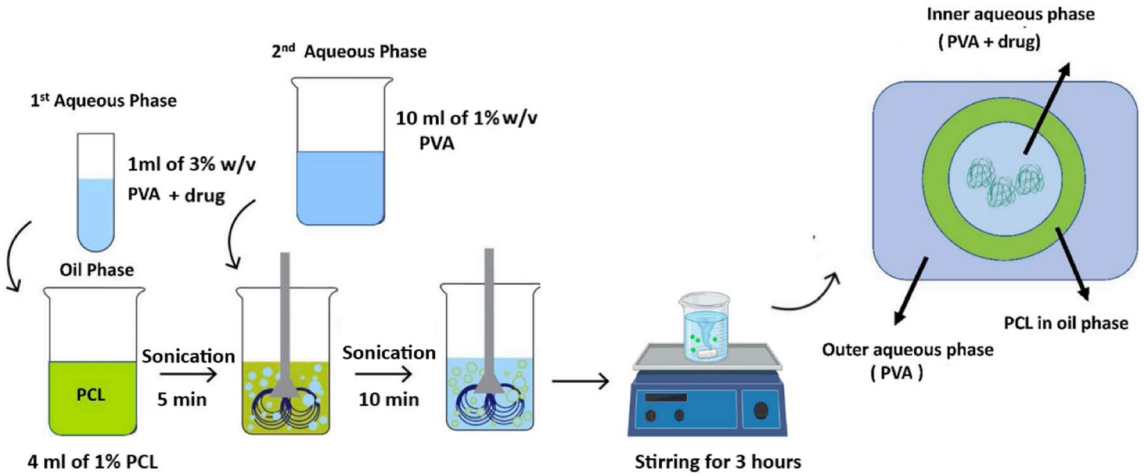

Fig. 1 Schematic representation of the fabrication technique of donepezil-loaded PCL/PVA NPs by the solvent evaporation technique. PVA: polyvinyl alcohol/PCL: polycaprolactone.

2.2. Preparation of DNP-loaded PCL/PVA nanoparticles

PCL/PVA NPs were prepared using the double-emulsion solvent evaporation technique, as described by Maatouk *et al.*[18] With slight modification as depicted in Fig. 1, PVA and PCL were dissolved in deionized water and dichloromethane to form clear aqueous (W1) and organic (O) solutions of concentrations 3% w/v and 1% w/v, respectively. The primary emulsion (W1/O) was formed by dispersing 1 mL of PVA solution in 4 mL of PCL solution using a probe sonicator equipped with a microtip (Q 700 sonicator, QSONICA, USA) at a frequency of 20 kHz and an amplitude of 20% for 5 min, with a 20-second on–off cycle. To produce the secondary emulsion (W1/O/W2), 10 mL of the second aqueous phase (W2), consisting of 1% w/v PVA, was added in a dropwise manner to the primary emulsion solution and sonicated for 10 minutes at an amplitude of 40%, with 20-s pulses on and 20-s pulses off. The obtained double emulsion was transferred into a container with a surface area of 2463 mm^2 and stirred on a magnetic stirrer at room temperature for a minimum of 3 hours to ensure the complete evaporation of DCM. Following synthesis, the NPs were centrifuged twice at 14 000 rpm for 20 minutes at 4 °C, with resuspension in deionized water between spins to remove any residual PVA or DCM. For the preparation of DNP-loaded PCL/PVA NPs, the same procedure was followed, but 10 mg of the drug was added initially to W1.

To fluorescently label PCL/PVA NPs, FITC-avidin was dissolved in the inner water phase (W1) before emulsification with the oil phase to form the primary W1/O emulsion. This allows for physical entrapment of the dye within the aqueous core of the resulting double emulsion (W1/O/W2). All subsequent steps were performed as described above. Successful encapsulation was quantitatively confirmed by fluorescence measurements, following repeated washing steps to remove non-encapsulated FITC-avidin from the external phase (W2). The apparent encapsulation efficiency, normalized to the total recovered dye, was determined to be 54.55 ± 4.68%.

2.3. Preparation of DNP-loaded DPPC-based liposomes

Liposomes were produced using the thin-film hydration method, followed by extrusion.[19] Chloroform was used to dissolve DPPC (25 mg mL^{-1}) and cholesterol (1 mg mL^{-1}) in a 1.6 : 1 molar ratio. The solution was placed on a vacuum pump (BOECO R-300, Hamburg, Germany) until the chloroform evaporated completely. The obtained thin film was then hydrated using 1 mL of deionized water warmed to 60 °C. The solution was left on a magnetic stirrer for 1 hour to form the liposomes (MUVs). Then, the liposome suspension was transferred to 1 mL gas-tight glass syringes (Hamilton, USA) for extrusion through the Avanti Mini-Extruder setup. Extrusion was sequentially performed 41 times through 100 nm polycarbonate membranes, with the setup placed on a heat block that had been previously heated to 60 °C. DNP-loaded liposomes were prepared in the same way; however, 10 mg of DNP was added to the 1 mL of deionized water before hydration of the thin film, as illustrated in Fig. 2. To fluorescently label DPPC-based liposomes, 0.3 mol% of rhodamine-labeled phosphatidylethanolamine (18 : 1 Liss Rhod PE, 1 mg mL^{-1} in chloroform) was mixed with DPPC and cholesterol before solvent evaporation.

2.4. Physicochemical characterization of DNP-loaded PCL/PVA nanoparticles and liposomal system

The particle size, polydispersity index, and zeta potential of the fabricated systems were determined by the Zetasizer 2000 (Malvern Instruments, Malvern, UK). The system was diluted at a 1 : 100 ratio with deionized water before being measured at room temperature and a scattering angle of 90°.[20]

To determine the entrapment efficiency (EE), the systems were centrifuged three times for 15 minutes at 5000 rpm using Amicon Ultra-4 centrifugal filters with a 3 kDa molecular weight cut-off (Merck, Germany). The supernatant was then collected, filtered, and diluted with deionized water to determine the free DNP using the UV-Vis mode of a NanoDrop 2000c

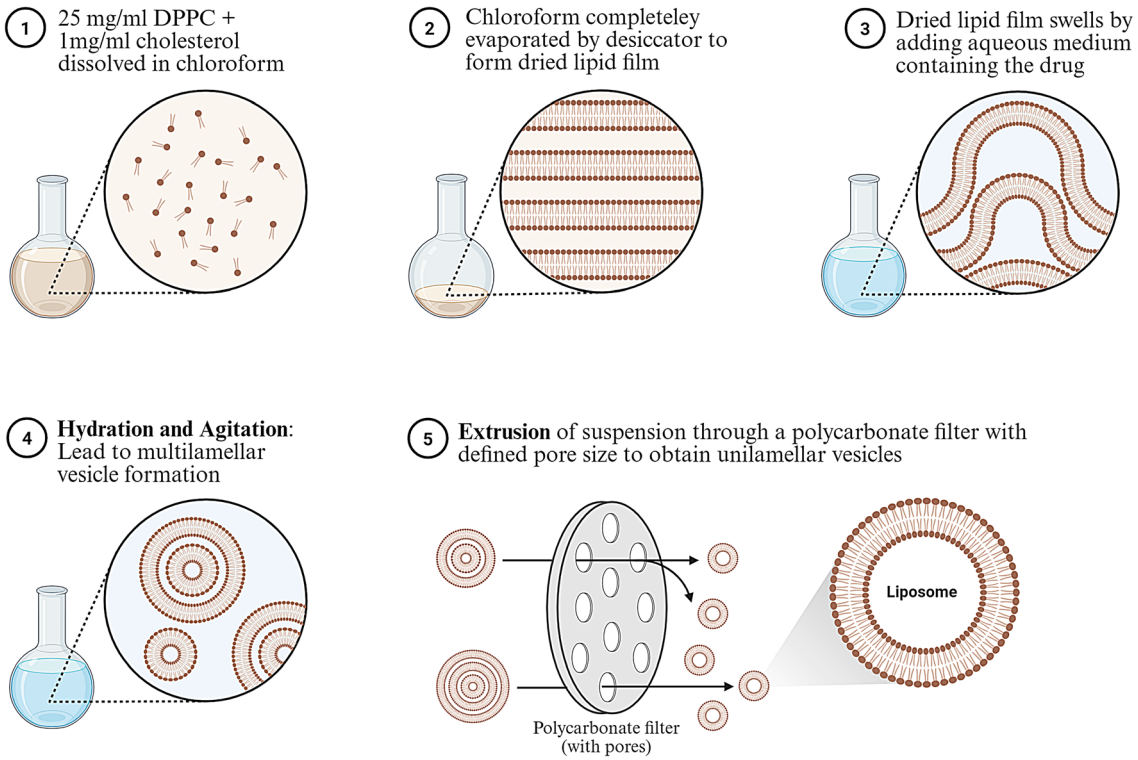

Fig. 2 Schematic representation of the fabrication technique of donepezil-loaded DPPC-based liposomes by the thin-film hydration technique, followed by extrusion.

spectrophotometer at a wavelength maximum (λ_{max}) of 271 nm (Thermo Scientific, Waltham, MA, USA). Entrapment efficiency was computed using the following equation:[21]

$$EE(\%) = \frac{\text{total amount of drug} - \text{free drug in the supernatant}}{\text{total amount of drug}} \times 100$$

The morphology of the DNP-loaded PCL/PVA NPs was determined using a scanning electron microscope (MIRA 3 TESCAN, Czechia) with the secondary electron detector, a voltage of 5.0 kV, and a working distance of 6–7 mm. The lyophilized polymeric NPs were placed on a metallic stub coated with a conductive double-sided adhesive carbon tape, followed by sputter coating with a 20 nm thick conductive gold layer using a Quorum 150 V Plus sputter coater (UK). In the case of liposomes, the system's morphology was visualized using a transmission electron microscope TEM (JOEL JEM CX 100 electron microscope). The system was diluted with ultra-pure water in a 1 : 1000 ratio. Then, drops from the diluted samples were placed on a copper grid, and the excess samples were removed using filter papers. The samples were stained with a uranyl acetate solution, and the grid was dried at room temperature before examination.[22]

Fourier transform infrared spectroscopy (FTIR) was employed to evaluate the state of DNP and the potential interaction between DNP and the system's components. An FTIR spectrometer was used to record the FTIR spectra of the raw drug, DNP, and the lyophilized DNP-loaded PCL/PVA double emulsion and liposomes at room temperature (Bruker Vector 42, Billerica, MA, USA). The samples were scanned over a range of 400–4000 cm^{-1} with 32 scans per sample to improve signal-to-noise ratio. Spectra were baseline corrected and normalized to allow comparability between samples.[23]

2.5. *In vitro* release study

Control (DNP in deionized water), 10 mL of PCL/PVA NPs, and 1 mL of DPPC-based liposomal dispersion, all containing an equivalent of 10 mg of DNP, were placed into dialysis bags with semi-permeable membranes (12 kDa molecular weight cut-off, Sigma-Aldrich, USA). The bags were pre-soaked overnight in deionized water and then immersed in beakers containing phosphate-buffered saline (pH 6.8).

The volume difference between the nanocarriers reflects formulation-specific handling considerations: polymeric nanoparticles were not further concentrated to avoid potential instability or aggregation, whereas liposomes were used at their native concentration, requiring a smaller volume to deliver an equivalent drug dose. Concentrating the PCL/PVA nanoparticle dispersion to substantially smaller volumes would increase solids content and viscosity, which may promote aggregation and affect dispersion stability. The free DNP solution in deionized water was used as a control for two purposes: (i) to establish a baseline for comparison and (ii) to verify that the dialysis membrane did not impose diffusion limitations,

thereby confirming that any observed sustained release was attributable to the formulation.

The bags were fully immersed in a sufficiently large volume of release medium to ensure sink conditions throughout the experiment at 38 ± 0.5 °C and stirred at 250 rpm. Samples were withdrawn at predetermined time intervals, and sink conditions were maintained by replacing the withdrawn volume with an equal volume of fresh release medium.[24] Under these conditions, drug release is governed primarily by the total drug amount rather than the internal formulation volume, allowing valid comparison between formulations. The withdrawn samples were assayed spectrophotometrically for DNP content at 271 nm using the UV-Vis mode of a NanoDrop 2000c spectrophotometer (Thermo Scientific, Waltham, MA, USA).

2.6. Cell studies

2.6.1. Cell culture. Human immortalized endothelial-like ECV-304 and neuronal-like PC-12 cell lines were used in this study, along with Roswell Park Memorial Institute (RPMI-1640) media for ECV-304 and Dulbecco's Modified Eagle Medium/Nutrient Mixture F-12 (DMEM/F-12, Ham) for PC-12 cells, both supplemented with 10% FBS and 1% penicillin–streptomycin. The cells were maintained in T-25 culture flasks and subcultured when they reached 80–90% confluence.

Upon entering systemic circulation, nanoparticles are expected to interact with vascular endothelial cells, which represent a key biological interface relevant to endothelial barrier transport processes associated with the BBB. To model these complex cellular interactions, we selected two established cell lines: ECV-304 for endothelial-like barrier studies and PC-12 for assessing neuronal uptake.

The ECV-304 cell line was selected for its endothelial-like properties and reported ability to form functional monolayers expressing tight junction proteins, including zonula occludens-1, occludin, and claudin-5.[25,26] These proteins localize at intercellular tight junctions and regulate paracellular transport, allowing discrimination between paracellular and transcellular transport pathways with different permeabilities.[26] We acknowledge that more physiologically relevant models, such as primary or iPSC-derived brain endothelial cells, better represent the BBB, including tight junction integrity and efflux transporter activity. However, these models are associated with high cost, limited availability, batch-to-batch variability, and technical complexity, which restricted their use in this initial proof-of-concept study. For the comparative objective of this work, the reproducibility, ease of culture, and cost-effectiveness of ECV-304 cells make them suitable for preliminary evaluation, although this model does not fully replicate the BBB.

For neuronal uptake assessment, PC-12 cells were employed due to their neuron-like properties and frequent use in neurodegenerative disease research to assess neuronal cell death and neurotoxic damage.[27] Our study specifically focused on evaluating nanoparticle internalization and cytotoxicity in these endothelial-like and neuronal-like cells, providing essential preliminary data on nanoparticle–endothelial and nanoparticle–neuron interactions.

2.6.2. PCL/PVA nanoparticles and DPPC-based liposomes safety profile using trypan blue exclusion assay. To evaluate the cytotoxicity of PCL/PVA NPs and DPPC-based liposomes, ECV-304 and PC-12 cells were each seeded in 48-well plates. The cells were cultured until they became 40–50% confluent. The culture medium was then replaced with fresh medium containing the prepared NPs at different concentrations of the drug, ranging from 3.125 to 50 μg mL^{-1} of DNP, in triplicate. The cells were incubated with the particles for 24, 48, and 72 h, and then the viability was measured at each time point. The cells were trypsinized and stained with trypan blue, and the % viability at each condition was then calculated and normalized against the control.

2.6.3. Qualitative and quantitative cellular uptake analysis. Fluorescence microscopy was used to visualize the cellular uptake of the two formulations. In brief, PC-12 and ECV-304 cells were seeded into 6-well plates at a density of 180 000 cells per well and incubated for 24 hours to allow attachment. The medium was then replaced with serum-free media appropriate for each cell line and incubated for an additional 24 hours to serum-starve the cells. Following starvation, FITC-labelled PCL/PVA NPs and rhodamine-labelled DPPC-based liposomes were added to their respective wells and incubated for another 24 hours. The medium was then removed, and the cells were washed thoroughly with PBS to remove surface-associated NPs. The cells were fixed with 4% paraformaldehyde, counterstained with DAPI at a concentration of 1 μg mL^{-1}, and visualized using a fluorescent microscope (DM6-B, Leica Microsystems, Wetzlar, Germany).[28]

For quantitative analysis, 8000 cells from each cell line were seeded into each well of a black Nunclon Delta Surface 96-well plate to minimize inter-well fluorescence interference. After an initial incubation period of 24 hours, the culture medium was replaced with serum-free medium to induce serum starvation. Following another 24 hours, the cells were treated with the appropriate freshly prepared fluorescently labelled NPs to avoid photobleaching and leakage, along with their respective free dye controls. Free dye controls were included for two reasons: (i) to quantify background fluorescence from non-specifically bound dye, and (ii) to confirm that enhanced cellular uptake was attributable to the nanoparticle-associated dye rather than the fluorophore-related artifacts.

After a 24-hour treatment period, the culture medium containing the NPs was collected and saved for analysis. The cells were then washed twice with 1× PBS, followed by lysis using 0.5% Triton X-100 for 15 minutes at room temperature.[29] The fluorescence of the cell lysate and the collected medium was measured separately using a Thermo Scientific™ Varioskan™ LUX multimode microplate reader (Thermo Fisher Scientific, Waltham, MA, USA).

The fluorescence intensity of the samples was measured using top optics with excitation/emission wavelengths of 560 nm and 583 nm for rhodamine, and 495 nm and 511 nm for FITC (5 nm bandwidth). Because fluorescence intensity was linearly correlated with dye concentration (R^2 = 0.9758 for rhodamine and R^2 = 0.9841 for FITC), relative fluorescence

$$\% \text{ Cellular uptake} = \frac{\text{fluorescence of cell lysate}}{\text{fluorescence of cell lysate} + \text{fluorescence of collected medium}} \times 100$$

units (RFU) were directly proportional to dye concentration. Therefore, RFU values were used without conversion to absolute concentration. The percentage of relative cellular uptake was calculated as follows:

Given that this ratio normalizes for differences in total fluorescence recovered, it allows relative comparison between different formulations, although intrinsic variations between fluorophores may still influence signal intensity. Therefore, comparisons between formulations are interpreted in terms of relative uptake trends rather than absolute quantitative differences.

2.7. Statistical analysis

Experiments were conducted in three independent trial sets, with each replicate including separate sample preparations. The results obtained from various experiments were expressed as the mean ± SD (standard deviation) or mean ± SEM (standard error of mean). Statistical analysis was performed using GraphPad Prism version 8.0.1, with a p-value < 0.05 considered statistically significant. For the stability study, a two-way ANOVA followed by Tukey's *post hoc* test was used to evaluate time-dependent changes within each formulation. The *in vitro* release data were fitted to zero-order, first-order, Higuchi, and Korsmeyer–Peppas drug release models using GraphPad Prism to gain a more detailed understanding of the drug release kinetics. The standard for selecting the most relevant model was based on a goodness-of-fit test. For cell viability, a two-way ANOVA followed by Tukey's *post hoc* test was applied at each time point independently to compare the effect of different formulations across different concentrations within each cell line. Lastly, the cellular uptake study was analyzed using a one-way ANOVA followed by Tukey's *post hoc* test to compare the uptake of liposomes and nanoparticles to their respective free dye controls.

3. Results and discussion

3.1. Preparation of DNP-loaded PCL/PVA double emulsion by solvent evaporation technique and DPPC-based liposomes by thin-film hydration followed by extrusion

Double emulsion can be used to prepare polymeric nanoparticles, which allow the controlled release of drugs soluble in the internal aqueous phase or dispersed within the polymeric matrix. The most commonly used method for double emulsion nanoparticle synthesis and encapsulation of active ingredients is the solvent evaporation technique. This method is considered superior to other methods (*e.g.*, nanoprecipitation and emulsion diffusion) due to its simplicity and convenient control over process parameters. This technique is particularly effective for encapsulating highly hydrophilic drugs, including proteins and peptides.[30] In this technique, homogenization is performed in two steps. In the first step, water-soluble drugs are incorporated into the inner aqueous phase (W1), while polymer- or lipophilic drugs are added to the oil phase (O). Both phases are homogenized by proper agitation to form the primary emulsion (W1/O). The primary emulsion is then emulsified with the outer aqueous phase (W2) to create a double emulsion (W1/O/W2). The formation of the double emulsion is followed by evaporation of the organic solvent from the dispersed phase, leading to polymer hardening and encapsulation of the active material within the nanoparticle matrix.[31] In the current investigation, polycaprolactone (PCL) and polyvinyl alcohol (PVA) were selected as the polymer components owing to their favorable safety profile, biodegradability, and compatibility with a wide range of drugs.[32]

Regarding liposome preparation, the thin-film hydration method followed by the extrusion technique was used. This method is widely utilized owing to its simplicity and cost-effectiveness. It involves forming a thin lipid film through solvent evaporation, followed by hydration to produce heterogeneous multilamellar vesicles. These vesicles are then passed through polycarbonate membranes during extrusion to yield homogeneous, uniformly sized unilamellar vesicles. This combination enables efficient encapsulation of diverse compounds, provides reasonable control over liposome size and lamellarity, ensures reproducibility, and facilitates scalability under sterile conditions. These features make it ideal for drug delivery applications requiring stable, biocompatible liposomes with controlled particle size.[33] In this work, DPPC, a major phospholipid component of pulmonary surfactant, was utilized due to its amphiphilic structure, which features hydrophilic head groups and hydrophobic palmitic acid tails. These properties facilitate the formation of stable bilayers that closely resemble biological membranes, making DPPC highly suitable for liposomal drug delivery systems. Besides, DPPC exhibits excellent stability and oxidation resistance compared to natural phospholipids, which enhances its utility in pharmaceutical formulations.[34] Cholesterol fills the gaps between the phospholipids within the bilayer, thereby increasing the packing density and minimizing passive drug leakage. Our DPPC-based liposomal formulation contains 38 mol% cholesterol, which falls within the 20–40 mol% range previously reported to optimize liposome stability, including promoting lipid condensation and ordered packing in DPPC monolayers.[35] This concentration was selected based on literature reports that this range balances membrane rigidity and cytotoxicity, as levels above 50 mol% have been associated with toxicity.[36,37]

3.2. Physicochemical characterization of DNP-loaded PCL/PVA nanoparticles and liposomal systems

DNP-loaded PCL/PVA NPs displayed a nanometric size of 175.97 ± 11.72 nm and a narrow polydispersity index (PDI) of 0.136 ± 0.022. This indicates that the amplitude was high enough to increase energy dissipation within the system, leading to a high cavity collapse pressure and the formation of small droplets from the dispersed phase.[38] Moreover, the small size and low PDI value of the NPs can be attributed to the rapid solvent evaporation, which causes immediate particle solidification with limited fusion and particle aggregation, as reported in previous studies.[24] Similarly, the average size of DNP-loaded DPPC-based liposomes was 115.18 ± 4.63 nm with a 0.080 ± 0.023 PDI value. This indicates that the small pore sizes of the membrane used in the extrusion technique yield liposomes with small sizes and narrower size distributions, as reflected by lower PDI values. This can be attributed to the uniform pore geometry, which imposes a consistent size cutoff, thereby limiting the presence of larger vesicles and reducing heterogeneity.[39] Both formulations exhibited a unimodal size distribution, indicating a homogeneous particle population as reflected in Fig. 3.

Nanoparticle size and PDI are key parameters influencing the biological fate of nanocarriers. This is mainly due to their small size, which provides a large interfacial surface area that amplifies drug permeation across biological barriers, albeit with certain limitations.[40] However, size-dependent limitations exist that may affect biodistribution and clearance kinetics. For instance, extremely small NPs (<6 nm) undergo rapid renal clearance, while large NPs (>600 nm) are prone to hepatic macrophage phagocytosis, resulting in reduced blood circulation time.[41] For systemic delivery, NPs in the 20–200 nm range strike a balance between avoidance of renal clearance and macrophage uptake, with studies showing optimal half-life for NPs near 100 nm.[41,42] Accordingly, the engineered lipid and polymeric NPs in this study fall within this favorable size range, suggesting reduced hepatic clearance and potential for endothelial interaction.

The low PDI values confirm a narrow size distribution, reflecting homogeneity and complete solubilization of the polymers, lipids, and drug. This maximizes DNP loading, reduces the probability of agglomeration, and augments therapeutic efficacy.[8] Relatedly, previous studies have suggested that nanoparticle size can influence interactions with biological barriers, including endothelial interfaces associated with the BBB.[43] However, such interpretations remain speculative in the context of the present study, as no direct permeability or BBB transport experiments were performed.

The zeta potential of NPs is a vital criterion owing to its ability to reflect the physical stability of DNP-loaded PCL/PVA NPs and DNP-loaded DPPC-based liposomes, in which zeta potential values around ±30 mV can provide a packed and significant energy barrier that limits droplets' coalescence.[6] The prepared polymeric NPs and liposomes displayed a negative charge of −22.66 ± 0.68 mV and −21.83 ± 1.55 mV, respectively, which is considered high enough to provide electrostatic stability for the prepared NPs. It has been suggested in the literature that surface charge can also influence interactions with biological membranes and may affect lymphatic transport pathways. In this context, the negative zeta potential of the nanoparticles could potentially be associated with enhanced intestinal lymphatic uptake, as anionic carriers have been reported to exhibit superior lymphatic targeting compared to their neutral or cationic counterparts.[44] It has also been hypothesized that such systems may reduce hepatic first-pass metabolism by entering intestinal lymphatics and subsequently draining into systemic circulation *via* the thoracic duct.[45] However, these biodistribution-related outcomes were not evaluated in the present study and require confirmation through future *in vivo* investigations.

A stability study was conducted over three weeks, during which both delivery systems were stored at 4 ± 0.5 °C and evaluated weekly for their particle size, PDI, and zeta potential. This was performed to assess the short-term physicochemical stability of the formulations under refrigerated storage conditions before biological evaluation. As shown in Fig. 4, there were no significant changes observed in particle size and PDI over the three weeks. Nevertheless, a significant change in zeta potential was observed for both systems ($p < 0.05$). This may be attributed to changes in the polymer surface chemistry, as polymeric NPs can undergo surface rearrangements or degradation, leading to

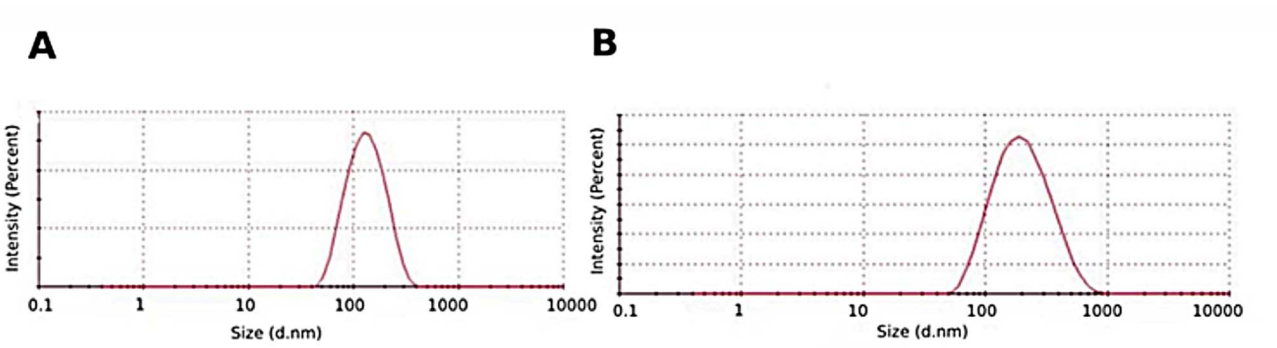

Fig. 3 Dynamic light scattering size distribution profiles of (A) donepezil-loaded DPPC-based liposomes and (B) donepezil-loaded PCL/PVA NPs. Both formulations exhibited unimodal size distribution.

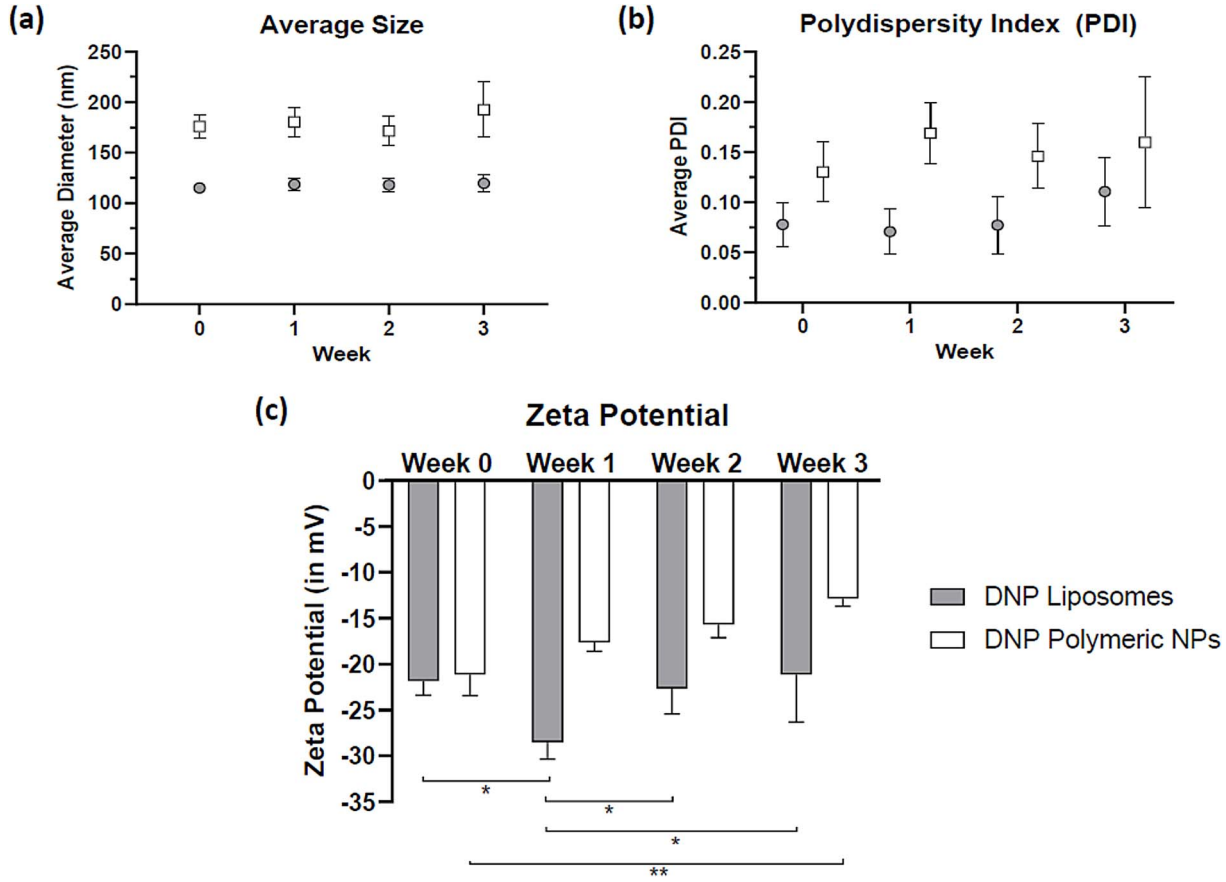

Fig. 4 Stability profiles of donepezil-loaded liposomes and donepezil-loaded PCL/PVA NPs concerning their (a) size, (b) polydispersity index, and (c) zeta potential. Results are expressed as mean standard deviation ± SD. Two-way ANOVA followed by a Tukey test was used to analyze changes over time for each formulation separately and denoted as follows: $p < 0.05$ (*) and $p < 0.01$(**).

alterations in the density and nature of charged functional groups on their surface, which directly affects the zeta potential.[14] In the case of liposomes, lipids and charged cholesterol may reorganize within the bilayer or partially desorb over time, resulting in changes in the surface charge and thus affecting the zeta potential.[46]

Entrapment efficiency (EE) refers to the percentage of the drug encapsulated within the NPs. This parameter indicates the effectiveness of drug incorporation into the carrier, which is crucial when assessing the physical properties of polymeric and lipid-based NPs. Furthermore, high EE significantly influences the rate of drug release, ensuring the high efficacy of the encapsulated drug at lower doses compared to its free counterpart administration, thereby minimizing the drug's toxic side effects.[21] The prepared PCL/PVA NPs and DPPC-based liposomes displayed an entrapment efficiency of 60.95 ± 6.03% and 88.55 ± 3.51% respectively, which indicates a good solubilization of DNP within the fabricated systems and the suitable coordination between the DNP and the systems components, confirming that DNP is well entrapped with a minimum chance of undesirable leakage.[47]

The ATR-FTIR spectra of the raw drug, DNP, DNP-loaded DPPC-based liposomes, and DNP-loaded PCL/PVA double emulsion were elucidated in Fig. 5. These spectra were performed to detect chemical compatibility and assess any potential interaction between excipients and the drug. The spectrum of the pure DNP drug (Fig. 5a) showed a characteristic peak corresponding to the CH group at 2923 cm^{-1}, C=O stretch at 1682 cm^{-1}, and an aryl C=C stretch at 1589 cm^{-1}. Moreover, a peak at 1499 cm^{-1} is attributed to N–H bending, and another peak at 1119 corresponds to C–O stretching. Finally, a peak was observed at 748 cm^{-1} due to C–H bending. For both DNP-loaded DPPC-based liposomes and DNP-loaded PCL/PVA NPs, the ATR-FTIR spectra revealed that the characteristic functional groups of DNP were retained, with no new peaks or bands observed. As a result, the presence of other excipients, such as PCL, PVA, DPPC, and cholesterol, did not affect the prominent DNP peaks, indicating that there were no chemical changes or interactions between the drug and the excipients used.

Morphological and structural features of DNP-loaded PCL/PVA NPs and DNP-loaded DPPC-based liposomes were examined utilizing SEM and TEM, respectively, as shown in Fig. 6. The micrograph displayed nano-droplets with smooth spherical outlines. Most droplets had a diameter of less than 200 nm, verifying the data recorded by the zeta sizer.

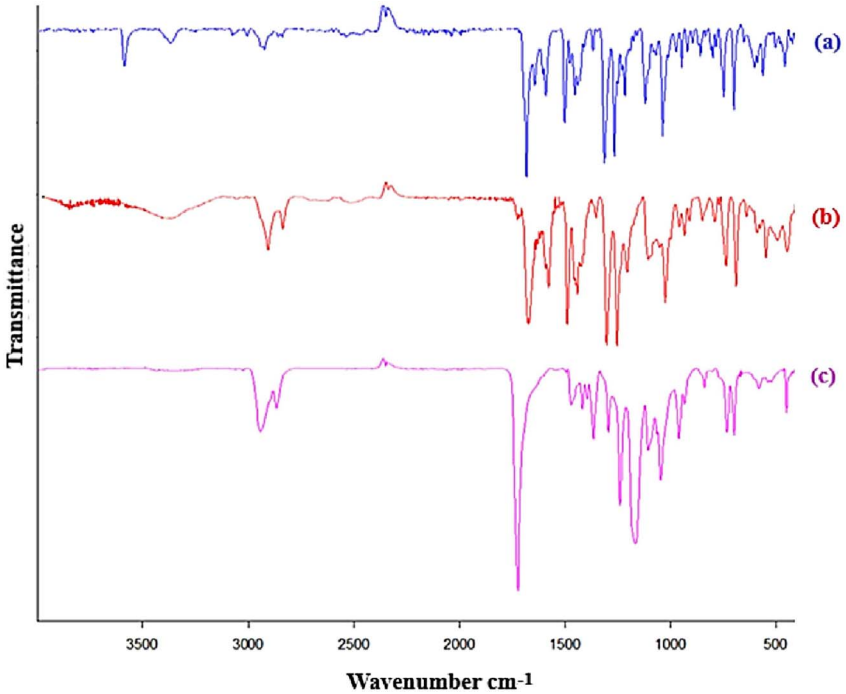

Fig. 5 Fourier transform infrared spectra of (a) raw donepezil powder, (b) lyophilized donepezil-loaded liposomes, and (c) lyophilized donepezil-loaded PCL/PVA nanoparticles. The results show no chemical or physical interaction between donepezil and the excipients used in either nanoparticle formulation.

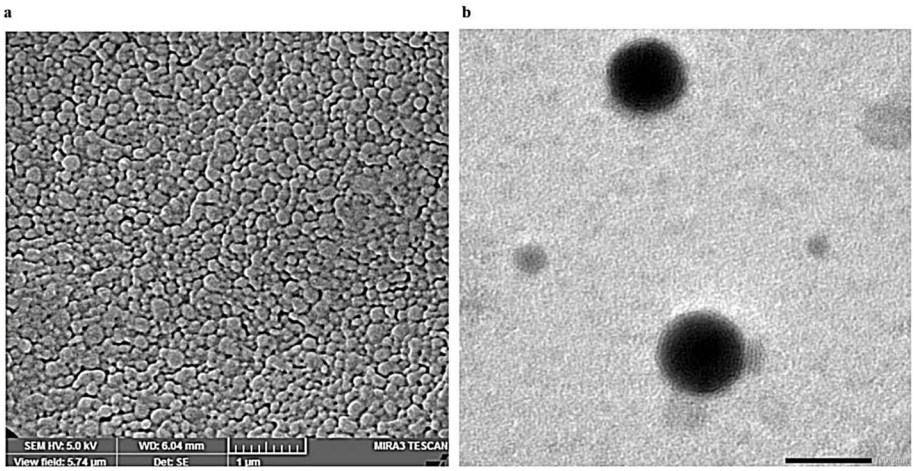

Fig. 6 (a) Scanning electron microscopy (SEM) image of donepezil-loaded PCL/PVA double emulsion nanoparticles showing spherical morphology and uniform size distribution. (b) Transmission electron microscopy (TEM) image of donepezil-loaded DPPC-based liposomes, revealing spherical, unilamellar vesicles with well-defined bilayer structures. Scales: 1 µm and 100 nm for SEM and TEM, respectively.

3.3. *In vitro* release study

The *in vitro* release study is vital because it provides critical information on the extent and rate of drug release from novel pharmaceutical formulations under controlled laboratory conditions, thereby mimicking physiological conditions to predict how the drug will behave in the body. Thus, an *in vitro* release study can reduce the need for extensive animal and human trials, streamline the regulatory approval process, and accelerate clinical translation.[48] The release of DNP from the formulated systems was assessed in triplicate. It was observed that the formulated systems were able to control and prolong the drug release over 48 hours (Fig. 7).

PCL/PVA NPs exhibited an initial burst release of approximately 40% in 3 hours, while liposomes released only around 18% of the encapsulated DNP within the same timeframe. This aligns with Alex *et al.*'s observations of carboplatin-loaded PCL nanoparticles, where burst release was attributed to surface-adsorbed drug dissolution.[49] In contrast, the control solution

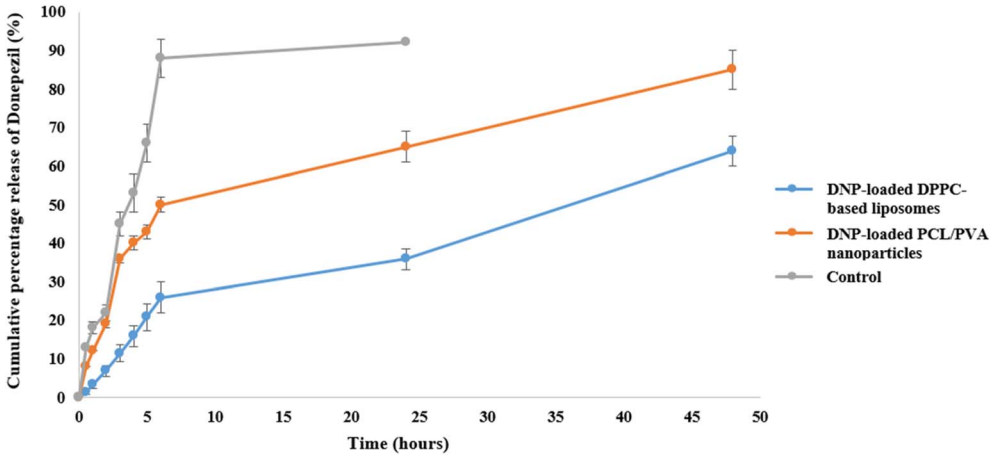

Fig. 7 *In vitro* release profiles of donepezil from control donepezil solution, donepezil-loaded PCL/PVA NPs, and donepezil-loaded DPPC-based liposomes over 48 hours into buffer saline (pH 6.8). The bags were fully immersed under conditions of 38 ± 0.5 °C. The control donepezil solution showed the fastest release. PCL/PVA NPs exhibited a biphasic release pattern: an initial burst followed by sustained release. DPPC-based liposomes demonstrated the most prolonged release.

showed a higher initial release of 53 ± 5.9% DNP within the first 4 hours. This can be mainly attributed to diffusion across the membrane into the dissolution medium, thereby confirming that the membrane did not limit the release rate.

Following the initial burst release from the polymeric NPs, both formulations exhibited a sustained biphasic release profile. This behavior may be associated with the efficient incorporation and solubilization of DNP within the polymeric and lipid systems, where surface-associated drug contributes to the initial burst, while the encapsulated fraction governs the prolonged release phase. Remarkably, DNP-loaded DPPC-based liposomes displayed more controlled release compared to PCL/PVA polymeric NPs. The polymeric NPs required approximately 6 hours to release 50% of the loaded DNP, while the liposomal system took around 16 hours, representing their respective release half-lives. These results may be attributed to the phospholipid bilayer structure of liposomes, which acts as a semi-permeable barrier that slows drug diffusion and reduces the initial burst release. Furthermore, literature has reported that the lipid barrier in liposomes or lipid–polymer hybrid nanoparticles significantly inhibits burst release and extends the time required to release a given amount of drug compared to pure polymer nanoparticles, confirming the superior controlled release properties of the liposomal system.[50]

The sustained release observed in the second phase of the biphasic release profile of the liposomal drug delivery system can also be attributed to the liposomal cholesterol content. Higher cholesterol concentrations in DPPC liposomes were found to decrease membrane fluidity and permeability, slowing drug diffusion and reducing the release rate, as reported in previous studies.[37,51] In line with these results, an earlier study demonstrated that liposomal formulations exhibited slower *in vitro* drug release compared to polymeric nanoparticles. The phospholipid bilayer structure of liposomes, along with cholesterol, serves as an effective barrier, reducing the initial burst release and allowing gradual diffusion of the encapsulated drug over extended periods. For example, gemcitabine-loaded liposomes displayed cumulative release profiles reaching approximately 90% over 24 hours, whereas poly(lactic-*co*-glycolic acid)-based NPs demonstrated a faster drug release attributed to polymer degradation and diffusion mechanisms.[52]

The ability of DPPC-based liposomes to sustain DNP release for 48 hours presents a possible therapeutic advantage. This extended release may allow less frequent dosing and more consistent drug concentrations, which is particularly important for long-term AD management, although further *in vivo* studies are needed to confirm these potential benefits.

The release of drugs from controlled delivery systems is influenced by the carrier matrix composition and drug–polymer interactions, with common mechanisms including diffusion, polymer relaxation, swelling, and erosion.[53] For this reason, the *in vitro* release data were fitted to zero-order, first-order, Higuchi, and Korsmeyer–Peppas kinetic models, and the results are presented in Table 1. These model fittings provide a mathematical description of the release behavior rather than direct mechanistic proof.

For PCL/PVA double emulsion NPs, the Korsmeyer–Peppas model provided the best fit (R^2 = 0.9328), with the Higuchi model showing a weaker fit (R^2 = 0.8612) compared to the Korsmeyer–Peppas model. This is consistent with the biphasic release pattern observed. For DPPC-based liposomes, the release profile showed a good correlation with both the Korsmeyer–Peppas model (R^2 = 0.9485) and the Higuchi model (R^2 = 0.9383), indicating that diffusion through the lipid bilayer is the dominant release-controlling process.

Drug release kinetics were less accurately described by the zero-order model for polymeric nanoparticles (R^2 = 0.7162) than for liposomes (R^2 = 0.8908), indicating that liposomes approach constant release more closely, consistent with their sustained release profile. A relatively better fit was obtained with the first-order model for both formulations (R^2 = 0.8294 for PCL/PVA

Table 1 Kinetic model parameters for donepezil release from PCL/PVA polymeric nanoparticles and DPPC-based liposomes

	PCL/PVA polymeric nanoparticles			DPPC-based liposomes		
Model	Coefficient of determination (R^2)	Release constant (k)	Release exponent (n)	Coefficient of determination (R^2)	Release constant (k)	Release exponent (n)
Zero-order	0.7162	1.493% h^{-1}	—	0.8908	1.217% h^{-1}	—
First-order	0.8294	0.1064 h^{-1}	—	0.8719	0.0232 h^{-1}	—
Higuchi	0.8612	14.12% $(\sqrt{h})^{-1}$	—	0.9383	8.453% $(\sqrt{h})^{-1}$	—
Korsmeyer–Peppas	0.9328	21.09% h^{-n}	0.368	0.9485	6.740% h^{-n}	0.572

NPs; R^2 = 0.8719 for DPPC-based liposomes), suggesting concentration-dependent release behavior consistent with prolonged release systems.

The release exponent n obtained from the Korsmeyer–Peppas model for PCL/PVA NPs was 0.368 (95% CI: 0.323 to 0.415), which is below 0.43. This suggests that drug release from PCL/PVA NPs follows a Fickian diffusion mechanism, where diffusion is the primary rate-limiting step under the studied conditions, with very limited contribution from polymer swelling or matrix erosion.[54] This can be attributed to the hydrophobic nature of PCL, which minimizes water uptake and undergoes negligible erosion, thereby preventing significant swelling or polymer chain rearrangement over the 48-hour release period.[55] On the other hand, the release exponent n for DPPC-based liposomes was 0.572 (95% CI: 0.508 to 0.642) which is above 0.43, implying that this liposomal system follows anomalous transport. This suggests that drug release is influenced by both diffusion and lipid bilayer-related processes. Our findings are consistent with a previous study where liposomes with 40 mol% cholesterol exhibited anomalous transport ($n > 0.5$), while liposomes with lower cholesterol (3.35 mol%) showed Fickian diffusion ($n \approx 0.5$).[56] Thus, the higher n value for liposomes compared to polymeric NPs suggests that the liposomal bilayer may introduce additional resistance to drug release, likely due to the combined effects of the phospholipid bilayer structure and the high cholesterol content, which modulates membrane fluidity and permeability.

3.4. Biocompatibility study

To study the safety profiles of the prepared delivery systems, a trypan blue assay was conducted. This widely utilized technique assesses cell viability by distinguishing live cells from nonviable cells. The principle is that live cells possess intact membranes that exclude the dye and remain unstained, whereas damaged cells take up the dye and appear blue under a microscope.[57] However, this assay does not capture the full metabolic activity or apoptotic responses of the cells. For this reason, future studies incorporating complementary assays, such as MTT or apoptosis-specific analyses, would provide a more comprehensive evaluation of the safety profile of these nanocarriers.

PC-12 cells are widely used as a neuronal model because they share numerous neuronal properties, such as the ability to synthesize and release neurotransmitters and to differentiate into neuron-like cells under nerve growth factor stimulation. These cells are instrumental in investigating endocytic pathways, such as clathrin-mediated endocytosis, which is a key mechanism for nanoparticle internalization.[58] In addition, ECV-304 serves as a model for evaluating nanoparticle interaction with endothelial barriers. Thus, PC-12 and ECV-304 cells provide complementary data on nanoparticle behavior at two relevant biological interfaces and were used to evaluate the effect of increasing concentrations of control NPs and DNP-loaded NPs, either in polymeric or DPPC-based liposomes.

As depicted in Fig. 8, both DNP-loaded PCL/PVA NPs and DNP-loaded DPPC-based liposomes show high biocompatibility with high cell viability above 80% for all concentrations, despite a significant decrease compared to the control group in cell viability of ECV-304 after treating with high concentrations of DNP-loaded DPPC-based liposomes (25 and 50 μg mL^{-1}). This indicates that all the ingredients used in the fabrication of the systems, including DPPC, cholesterol, PCL, and PVA, did not exhibit any significant toxic effects on ECV-304 and PC-12 cell lines. The slight reduction in cell viability at high DPPC concentration can be attributed to the lipid–cholesterol saturation, which induces membrane rigidity and cumulative metabolic stress over extended exposure. This aligns with broader liposome toxicology principles where neutral lipids like DPPC cause concentration- and time-dependent cytotoxicity beyond threshold levels.[36] Further ECV-304-specific studies quantifying lipid accumulation and membrane dynamics would clarify the exact pathways.

3.5. Cellular uptake study

In vitro cellular uptake studies are crucial for evaluating the efficiency of novel drug delivery systems for cellular internalization. These studies provide data on the amount of the loaded cargoes that can be internalized, which directly impacts the treatment's effectiveness. By assessing *in vitro* internalization, scientists can design and compare novel formulations, thereby improving drug delivery and therapeutic outcomes. Furthermore, *in vitro* uptake data help predict the potential *in vivo* performance of the delivery system, thereby reducing the need for extensive animal testing. Hence, cellular uptake studies are a vital step in the preclinical evaluation of nanocarriers, ensuring their suitability for effective drug delivery.[59] In the current study, liposomes were labelled with rhodamine, and polymeric nanoparticles were labelled with FITC. Their uptake

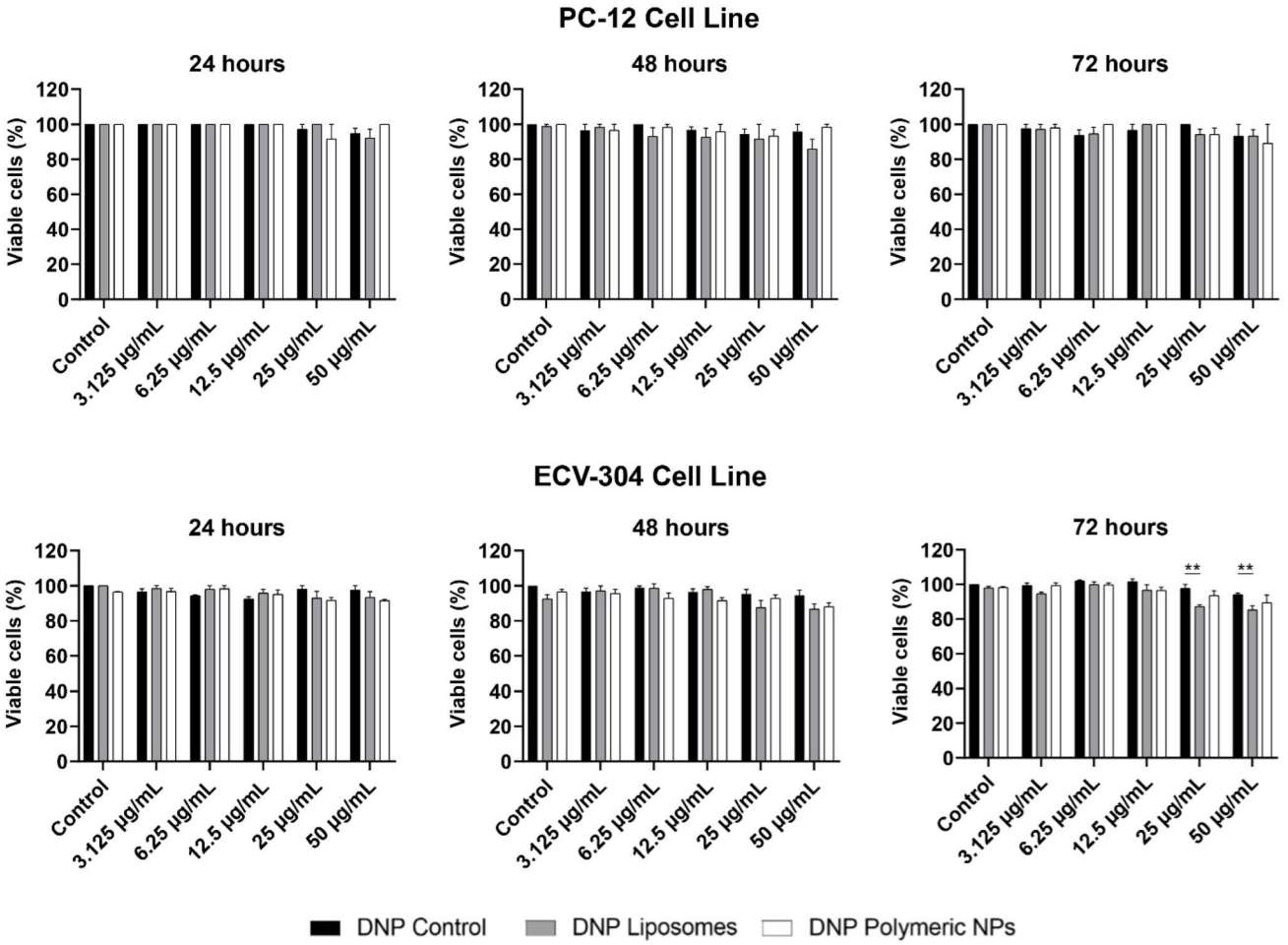

Fig. 8 Effects of donepezil control solution, donepezil-loaded polymeric NPs, and donepezil-loaded DPPC-based liposomes treatment on ECV-304 and PC-12 cells. Cells were treated with increasing concentrations (3.125–50 μg mL^{-1}) of each formulation in a time-dependent manner. All formulations maintained cell viability above 80% at concentrations up to 50 μg mL^{-1} in both cell lines, indicating acceptable biocompatibility. A Two-way ANOVA followed by Tukey's test was applied at each time point independently to compare the effect of different formulations across different concentrations within each cell line. **Significant with respect to the control ($p < 0.01$), as shown by two-way ANOVA. The data is reported as mean ± SEM ($n = 3$).

by the endothelial cell line ECV-304 and the neuronal-like cell line PC-12 was then analyzed. After 24 hours of incubation, cells were observed qualitatively using a fluorescence microscope. As illustrated in Fig. 9, both PCL/PVA NPs and DPPC-based liposomes were internalized by ECV-304 and PC-12 and localized around the nucleus, revealing their ability to penetrate the endothelial and neural cell membranes to deliver DNP into the cells.

For a deeper and more precise comparison between PCL/PVA NPs and DPPC-based liposomes, quantitative analysis was performed, as depicted in Fig. 10. This technique enables accurate measurement of internalized liposomes, thereby overcoming the limitations of the qualitative approach. The percentage of fluorescence inside and outside the cells was quantified using a microplate reader. As shown in Fig. 10, both delivery systems exhibited significantly improved cellular uptake in both cell lines compared to their respective free dye control. This behavior may be attributed to the ability of the nanoparticles to enter ECV-304 and PC-12 cells through endocytic pathways, given their small particle sizes. Clathrin-mediated or caveolae-mediated endocytosis may contribute to cellular uptake; however, this remains speculative, as no pathway-specific inhibition studies were performed to confirm the mechanism. Indeed, the average diameters of clathrin-coated and caveolae-coated vesicles are between 100 and 200 nm, representing the maximum size of NPs that can be internalized *via* these mechanisms.[60]

PCL/PVA NPs showed 27.41 ± 2.38% ECV-304 cellular uptake, which is significantly higher than that shown by 19.10 ± 3.58% DPPC-based liposomes ($p = 0.0425$). Additionally, PCL/PVA NPs exhibited higher PC-12 cellular uptake, at 35.10 ± 3.28%, compared to the liposomal system, at 28.81 ± 4.85% ($p = 0.1963$). The improved cellular uptake of PCL/PVA NPs compared to liposomes can be attributed to the structural properties of the polymeric nanoparticles, which generally promote more efficient internalization by cells. Unlike the relatively "soft" and fluid nature of liposomal membranes, polymeric nanoparticles tend to be more rigid and stable, which

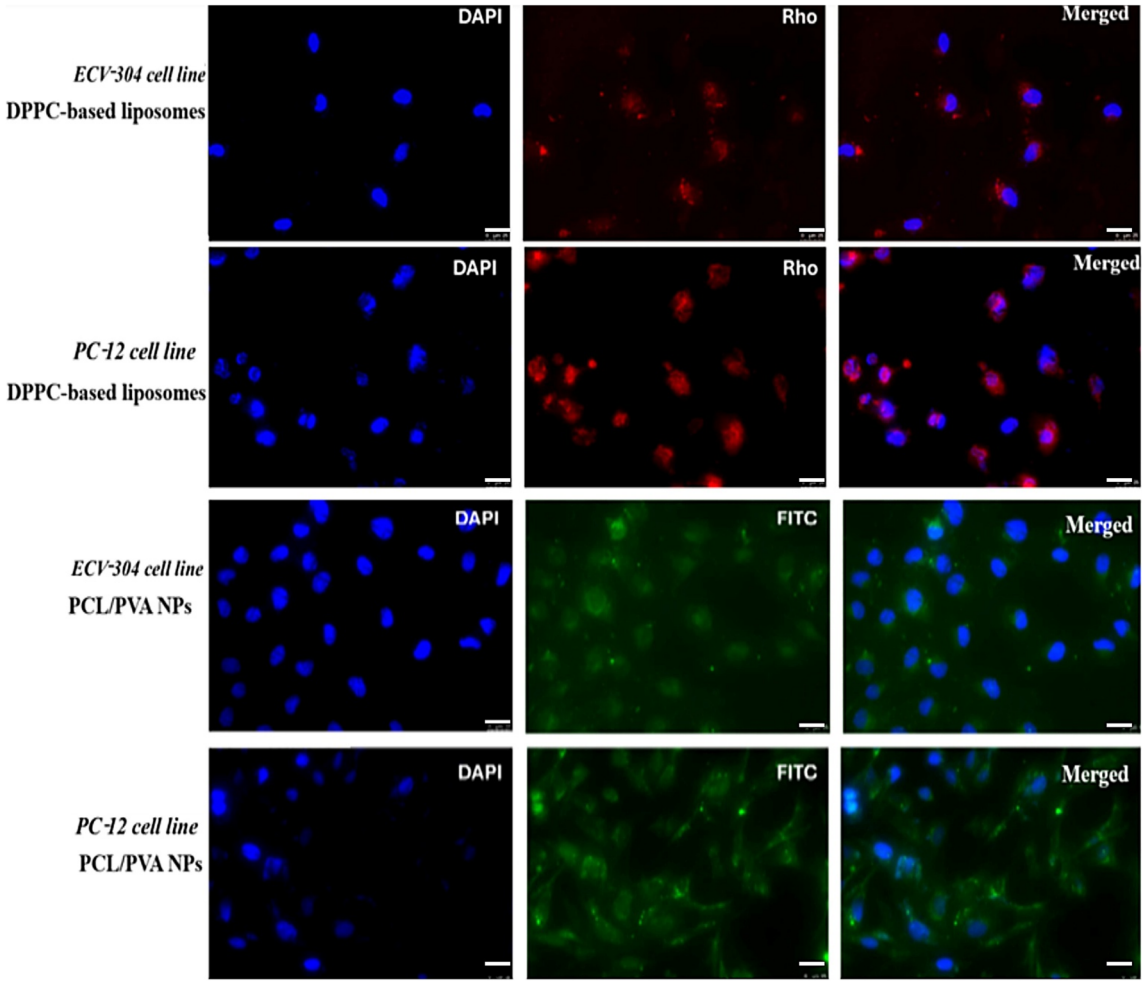

Fig. 9 *In vitro* cellular uptake of Rhodamine labelled DPPC-based liposomes (red) and FITC-labelled PCL/PVA nanoparticles (green) by ECV-304 and PC-12 cells after 24 hours of incubation period. Co-localization of the red fluorescence (liposomes) or green fluorescence (PCL/PVA NPs) in proximity to the blue DAPI-stained nuclei confirms the association of nanoparticles with ECV-304 and PC-12 cells, demonstrating either internalization or surface binding. Fluorescence microscopy was performed at 50× magnification; scale bar = 25 μm (consistent across all images).

can facilitate better interaction with the cellular environment and enhance uptake.[61] Furthermore, polymeric nanoparticles may exhibit greater stability under physiological conditions, leading to improved retention and accumulation within cells during *in vitro* studies.[62] These factors might explain the typically higher uptake levels observed for polymeric carriers compared to liposomes, independent of size or charge considerations.

Notably, there is a significant difference in the uptake of DPPC-based liposomes between the two different ECV-304 and PC-12 cell lines (p-value 0.0135 for DPPC-based liposomes; non-significant for PCL/PVA NPs, $p = 0.0698$). This could be attributed to differences in cellular uptake mechanisms between distinct cell types. For instance, endothelial cells possess tight junctions that limit the penetration of nanoparticles and paracellular movement. It has been reported that nanoparticle uptake in endothelial cells may occur *via* caveolae-dependent endocytosis.[63,64] In contrast, neuronal cells have been reported to rely on clathrin-mediated endocytosis for nanoparticle uptake as they lack caveolae-1 protein.[64] However, these interpretations remain speculative, as pathway-specific inhibition studies were not conducted to confirm the mechanisms. Future studies must focus on identifying diverse mechanistic pathways to optimize nanoparticle design and therapeutic delivery across different cell types. A similar result was obtained in the Aibani *et al.* study, in which polymer-based nanoparticles demonstrated improved cellular uptake compared to corresponding liposomes.[65]

It is important to acknowledge that cellular internalization does not necessarily lead to improved therapeutic efficiency, as this depends on the ability of nanocarriers to escape endosomes. Since this was not the aim of the present study, we did not quantify the fraction of DNP released into the cytosol *versus* that trapped in endosomes or lysosomes. Future studies employing fluorescent probes that sense endosomal escape are needed to assess whether nanocarrier composition influences cytosolic delivery of DNP.

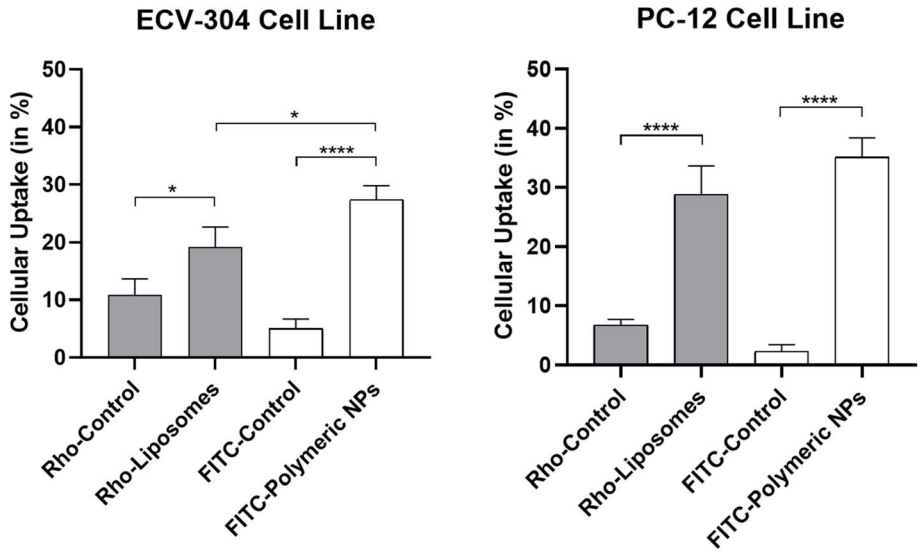

Fig. 10 Quantitative analysis of cellular uptake of rhodamine-labelled DPPC-based liposomes and FITC-labelled PCL/PVA NPs along with their respective free dye controls by ECV-304 and PC-12 cell lines. Both formulations showed significantly higher uptake than their respective free dye controls. PCL/PVA nanoparticles exhibited significantly higher uptake than liposomes in ECV-304 cells. Results are expressed as mean ± SD. Statistical significance was determined using a one-way ANOVA followed by Tukey's test to compare liposomes and nanoparticles uptake against their respective controls and denoted as follows: $P < 0.05$ (*), $p < 0.01$ (**), $p < 0.001$ (***), $p < 0.0001$ (****).

The results of this study suggest a possible trade-off between drug release kinetics and cellular uptake. As discussed above, DPPC-based liposomes exhibited more controlled drug release over 48 hours but showed lower cellular uptake in both ECV-304 and PC-12 cells. In contrast, PCL/PVA polymeric NPs had faster release but demonstrated significantly higher cellular uptake. This observation suggests that formulation parameters such as drug encapsulation and release behavior do not necessarily predict cellular internalization efficiency under the tested *in vitro* conditions. For brain delivery, both systems may offer distinct advantages. The higher cellular uptake of polymeric nanoparticles may support improved intracellular delivery in cell-based models, while the sustained release profile of liposomes may prolong drug availability and reduce dosing frequency, which is relevant for chronic diseases like AD. Thus, neither formulation appears universally superior, and the optimal choice may depend on the intended therapeutic objective. Future studies could explore hybrid lipid–polymer nanoparticles that combine the favorable release properties of liposomes with the higher cellular uptake of polymeric nanoparticles for potential brain delivery applications.

4. Conclusion and outlook

In summary, DNP-loaded DPPC-based liposomes and PCL/PVA-based polymeric nanoparticles were successfully fabricated using thin film hydration and solvent evaporation techniques, respectively, for potential application in Alzheimer's disease. The mean particle sizes of polymeric nanoparticles and liposomes were 175.97 ± 11.72 nm and 115.18 ± 4.63 nm, respectively, with narrow size distributions (PDI < 0.3) and favorable physicochemical properties. Both systems exhibited good biocompatibility, maintaining over 80% cell viability across the tested concentrations. DPPC-based liposomes demonstrated more sustained drug release over 48 hours ($t_{1/2} \approx 16$ h) compared to the polymeric nanoparticle ($t_{1/2} \approx 6$ h). In contrast, both formulations showed enhanced cellular uptake relative to their respective controls, with PCL/PVA nanoparticles exhibiting higher uptake, highlighting a trade-off that should guide formulation design for CNS applications.

This work represents an incremental contribution by showing that carrier composition alone, without targeting ligands or surface modifications, significantly influences release kinetics and cellular uptake by neuronal and endothelial cells. Future studies could explore polymer–lipid hybrid nanoparticles that combine the high cellular uptake of polymeric systems with the sustained release properties of liposomes. In addition, assessing the endosomal escape of DNP would provide further insight into intracellular drug delivery. Such studies could help delineate the mechanisms by which cell line-specific properties govern uptake efficiency across distinct neuronal and endothelial cell types. Further investigation should extend into *in vivo* studies to evaluate the potential of these systems for brain delivery applications.

Author contributions

Kawthar K. Abla and Toros Torossian: methodology, investigation, data curation, and conceptualization. Jana Dakour and Sara Assi: formal analysis and data curation. Mia Karam: software. Jana Dakour: validation, methodology. Rami Mhanna: supervision.

Conflicts of interest

The authors declare that they have no known competing financial interests or personal relationships that could have influenced the work reported in this paper.

Data availability

The authors confirm that the data supporting the findings of this study are available within the article. Raw files supporting the findings of this study are available from the corresponding author on request.

Acknowledgements

We are greatly indebted to the Kamal A. Shair Central Research Science Laboratory at the American University of Beirut (AUB) and the Nano-technology Research Lab at Beirut Arab University (BAU) for providing the essential equipment and facilities required to characterize the synthesized nanoparticles. This work was also supported by the University Research Board (URB) and by Vertically Integrated Projects Program (VIP).

References

1 K. K. Abla and M. K. Zahwi, *J. Drug Delivery Sci. Technol.*, 2024, **102**, 106409.
2 Alzheimer's Association, *Alzheimer's Dement.*, 2025, **21**, e70235.
3 M. R. Peltier and M. Sofuoglu, in *Cognition and Addiction*, ed. A. Verdejo-Garcia, Academic Press, 2020, pp. 303–320, DOI: 10.1016/B978-0-12-815298-0.00023-X.
4 R. Oliveira Silva, H. Counil, J. M. Rabanel, M. Haddad, C. Zaouter, M. R. Ben Khedher, S. A. Patten and C. Ramassamy, *Int. J. Nanomed.*, 2024, **19**, 1077–1096.
5 Y. B. Ji, S. Lee, H. J. Ju, H. E. Kim, J. H. Noh, S. Choi, K. Park, H. B. Lee and M. S. Kim, *J. Controlled Release*, 2023, **356**, 43–58.
6 M. M. Mehanna, K. K. Abla, S. Domiati and H. Elmaradny, *Int. J. Pharm.*, 2022, **622**, 121830.
7 K. K. Abla, M. K. Alamoudi, G. A. Soliman, M. S. Abdel-Kader, M. F. Aldawsari and M. M. Mehanna, *Int. J. Nanomed.*, 2025, **20**, 605–624.
8 K. K. Abla, S. Domiati, R. El Majzoub and M. M. Mehanna, *Gels*, 2023, **9**, 491.
9 K. K. Abla and M. M. Mehanna, *J. Drug Targeting*, 2023, **31**, 832–857.
10 Z. Q. Zhao, B. Z. Chen, X. P. Zhang, H. Zheng and X. D. Guo, *Mol. Pharm.*, 2021, **18**, 2482–2494.
11 D. Wang, Q. Jiang, Z. Dong, T. Meng, F. Hu, J. Wang and H. Yuan, *Adv. Drug Delivery Rev.*, 2023, **203**, 115130.
12 J. Ahlawat, G. Guillama Barroso, S. Masoudi Asil, M. Alvarado, I. Armendariz, J. Bernal, X. Carabaza, S. Chavez, P. Cruz, V. Escalante, S. Estorga, D. Fernandez, C. Lozano, M. Marrufo, N. Ahmad, S. Negrete, K. Olvera, X. Parada, B. Portillo, A. Ramirez, R. Ramos, V. Rodriguez, P. Rojas, J. Romero, D. Suarez, G. Urueta, S. Viel and M. Narayan, *ACS Omega*, 2020, **5**, 12583–12595.
13 Y. H. Song, R. De and K. T. Lee, *Adv. Colloid Interface Sci.*, 2023, **320**, 103008.
14 A. Zielińska, F. Carreiró, A. M. Oliveira, A. Neves, B. Pires, D. N. Venkatesh, A. Durazzo, M. Lucarini, P. Eder, A. M. Silva, A. Santini and E. B. Souto, *Molecules*, 2020, **25**, 3731.
15 S. M. Bhavna, M. Ali, S. Baboota, J. K. Sahni, A. Bhatnagar and J. Ali, *Drug Dev. Ind. Pharm.*, 2014, **40**, 278–287.
16 K. V. Krishna, G. Wadhwa, A. Alexander, N. Kanojia, R. N. Saha, R. Kukreti, G. Singhvi and S. K. Dubey, *ACS Chem. Neurosci.*, 2019, **10**, 4124–4135.
17 K. K. Abla, T. Torossian, J. Ammar, M. Karam, M. Fawaz, R. Debian, M. Mehanna, A. Daou and R. Mhanna, *Int. J. Biol. Macromol.*, 2025, **332**, 148548.
18 B. Maatouk, M. A. Jaffa, M. Karam, D. Fahs, W. Nour-Eldine, A. Hasan, A. A. Jaffa and R. Mhanna, *Colloids Surf., B*, 2021, **208**, 112105.
19 A. Cazzolla, J. R. M. Mondala, J. Wanigasekara, J. Carroll, N. Daly, B. Tiwari, A. Casey and J. F. Curtin, *PLoS One*, 2024, **19**, e0300467.
20 K. K. Abla, A. T. Mneimneh, A. N. Allam and M. M. Mehanna, *Pharmaceutics*, 2023, **15**, 173.
21 K. K. Abla, S. M. Hijazi and M. M. Mehanna, *J. Drug Delivery Sci. Technol.*, 2023, **87**, 104764.
22 M. M. Mehanna, K. K. Abla and H. A. Elmaradny, *Adv. Pharm. Bull.*, 2021, **11**, 274–285.
23 A. T. Mneimneh, B. Hayar, S. Al Hadeethi, N. Darwiche and M. M. Mehanna, *Pharmaceutics*, 2025, **17**, 698.
24 W. Guo, P. Quan, L. Fang, D. Cun and M. Yang, *Asian J. Pharm. Sci.*, 2015, **10**, 405–414.
25 S. Yang, H. Jin and Z. Zhao, *Neurol. Res.*, 2018, **40**, 117–121.
26 S. Yang, S. Mei, H. Jin, B. Zhu, Y. Tian, J. Huo, X. Cui, A. Guo and Z. Zhao, *PLoS One*, 2017, **12**, e0187017.
27 D. Xie, T. Deng, Z. Zhai, T. Sun and Y. Xu, *Front. Mol. Neurosci.*, 2023, **15**, 1016559.
28 M. Shi, X. Zhao, J. Zhang, S. Pan, C. Yang, Y. Wei, H. Hu, M. Qiao, D. Chen and X. Zhao, *Int. J. Nanomed.*, 2018, **13**, 6885–6902.
29 H. J. Shin, M. Kwak, S. Joo and J. Y. Lee, *Sci. Rep.*, 2022, **12**, 20146.
30 M. Iqbal, N. Zafar, H. Fessi and A. Elaissari, *Int. J. Pharm.*, 2015, **496**, 173–190.
31 T. K. Giri, C. Choudhary, Ajazuddin, A. Alexander, H. Badwaik and D. K. Tripathi, *Saudi Pharm. J.*, 2013, **21**, 125–141.
32 N. A. Pattanashetti, D. D. Achari, A. I. Torvi, R. V. Doddamani and M. Y. Kariduraganavar, *Materialia*, 2020, **12**, 100826.
33 V. V. S. N. L. Andra, S. V. N. Pammi, L. V. K. P. Bhatraju and L. K. Ruddaraju, *BioNanoScience*, 2022, **12**, 274–291.
34 A. Najm, A. C. Bîrcă, A.-G. Niculescu, A. Alberts, A. M. Grumezescu, B. Gălăţeanu, B. Ş. Vasile, M. Beuran, B. S. Gaspar and A. Hudiţă, *Molecules*, 2025, **30**, 1437.
35 T. Yokoyama, D. Yoshida, H. Mori, M. Okabe, Z. Shervani, K. Taga, Y. Yamamoto, A. Sumino, T. Dewa, M. Nango and M. Yamamoto, *J. Biophys. Chem.*, 2016, **7**, 98–109.

36 C. T. Inglut, A. J. Sorrin, T. Kuruppu, S. Vig, J. Cicalo, H. Ahmad and H.-C. Huang, *Nanomaterials*, 2020, **10**, 190.
37 S. Kaddah, N. Khreich, F. Kaddah, C. Charcosset and H. Greige-Gerges, *Food Chem. Toxicol.*, 2018, **113**, 40–48.
38 E. Ruiz, V. H. Orozco, L. M. Hoyos and L. F. Giraldo, *Eur. Polym. J.*, 2022, **173**, 111307.
39 S. G. M. Ong, M. Chitneni, K. S. Lee, L. C. Ming and K. H. Yuen, *Pharmaceutics*, 2016, **8**, 36.
40 S. Gorantla, V. K. Rapalli, T. Waghule, P. P. Singh, S. K. Dubey, R. N. Saha and G. Singhvi, *RSC Adv.*, 2020, **10**, 27835–27855.
41 M. Haripriyaa and K. Suthindhiran, *Future J. Pharmaceut. Sci.*, 2023, **9**, 113.
42 B. Lu, J. Wang, A. J. Hendriks and T. M. Nolte, *Environ. Sci.: Nano*, 2024, **11**, 406–417.
43 G. P. Hoyos-Ceballos, B. Ruozi, I. Ottonelli, F. Da Ros, M. A. Vandelli, F. Forni, E. Daini, A. Vilella, M. Zoli, G. Tosi, J. T. Duskey and B. L. López-Osorio, *Pharmaceutics*, 2020, **12**, 72.
44 A. Ali Khan, J. Mudassir, N. Mohtar and Y. Darwis, *Int. J. Nanomed.*, 2013, **8**, 2733–2744.
45 Y.-B. Miao, T. Xu, Y. Gong, A. Chen, L. Zou, T. Jiang and Y. Shi, *J. Nanobiotechnol.*, 2023, **21**, 263.
46 Z. Németh, I. Csóka, R. Semnani Jazani, B. Sipos, H. Haspel, G. Kozma, Z. Kónya and D. G. Dobó, *Pharmaceutics*, 2022, **14**, 1798.
47 Y. Li, S. Ruan, Z. Wang, N. Feng and Y. Zhang, *Pharmaceutics*, 2021, **13**, 1235.
48 J. Song, Z. Xu, L. Xie and J. Shen, *Pharmaceutics*, 2025, **17**, 256.
49 A. T. Alex, A. Joseph, G. Shavi, J. V. Rao and N. Udupa, *Drug Delivery*, 2016, **23**, 2144–2153.
50 S. Parveen, P. Gupta, S. Kumar and M. Banerjee, *Med. Drug Discov.*, 2023, **20**, 100165.
51 M.-L. Briuglia, C. Rotella, A. McFarlane and D. A. Lamprou, *Drug Delivery Transl. Res.*, 2015, **5**, 231–242.
52 T. E. Yalcin, S. Ilbasmis-Tamer, B. Ibisoglu, A. Özdemir, M. Ark and S. Takka, *Pharm. Dev. Technol.*, 2018, **23**, 76–86.
53 J. Siepmann and F. Siepmann, *Int. J. Pharm.*, 2008, **364**, 328–343.
54 L. Ahmed, R. Atif, T. Eldeen, I. Yahya, A. Omara and M. Eltayeb, *Int. J. Latest Technol. Eng. Manag. Appl. Sci.*, 2019, **8**, 52–56.
55 J. C. Jeong, J. Lee and K. Cho, *J. Contr. Release*, 2003, **92**, 249–258.
56 M. C. García, N. Naitlho, J. M. Calderón-Montaño, E. Drago, M. Rueda, M. Longhi, A. M. Rabasco, M. López-Lázaro, F. Prieto-Dapena and M. L. González-Rodríguez, *Pharmaceutics*, 2021, **13**, 973.
57 W. Strober, *Current Protocols in Immunology*, 2015, vol. 111, pp. A3.B.1–A3.B.3.
58 J. Liu, T. Wang, J. Dong and Y. Lu, *J. Nanobiotechnol.*, 2025, **23**, 146.
59 T. B. Gandek, L. van der Koog and A. Nagelkerke, *Adv. Healthcare Mater.*, 2023, **12**, 2300319.
60 K. K. Abla and M. M. Mehanna, *J. Controlled Release*, 2023, **362**, 70–96.
61 P. Foroozandeh and A. A. Aziz, *Nanoscale Res. Lett.*, 2018, **13**, 339.
62 S. Lazzari, D. Moscatelli, F. Codari, M. Salmona, M. Morbidelli and L. Diomede, *J. Nanopart. Res.*, 2012, **14**, 920.
63 S. Behzadi, V. Serpooshan, W. Tao, M. A. Hamaly, M. Y. Alkawareek, E. C. Dreaden, D. Brown, A. M. Alkilany, O. C. Farokhzad and M. Mahmoudi, *Chem. Soc. Rev.*, 2017, **46**, 4218–4244.
64 N. D. Donahue, H. Acar and S. Wilhelm, *Adv. Drug Delivery Rev.*, 2019, **143**, 68–96.
65 N. Aibani, T. N. Khan and B. Callan, *Int. J. Pharm.: X*, 2020, **2**, 100040.